

Poly(phenylenesulfide)-based coatings for carbon steel heat exchanger tubes in geothermal environments

T. SUGAMA, D. ELLING

*Energy Resources Division, Energy Science & Technology Department,
Brookhaven National Laboratory, Upton, NY 11973, USA
E-mail: sugama@bnl.gov*

K. GAWLIK

National Renewable Energy Laboratory, 1617 Cole Boulevard, Golden, Colorado 80401, USA

To inhibit corrosion and fouling by calcium silicate and silica scales of the carbon steel heat exchanger tubes in geothermal power plants operating at brine temperature of 160°C, their internal surfaces were lined with high-temperature performance poly(phenylenesulfide) (PPS)-based coating systems. The systems included the PPS containing polytetrafluoroethylene (PTFE) as an anti-oxidant additive, silicon carbide (SiC) as a thermally conductive filler, and aluminum oxide-rich calcium aluminate (ACA) as an abrasive wear resistant filler. Then, the lined tubes underwent an eleven-month-long field exposure at the site of power plant. The results from the post-test analyses of the exposed liners revealed that these PPS coating systems had an excellent thermal stability, and satisfyingly withstood this brine temperature, and also greatly resisted the permeation of brine, demonstrating that they adequately protect the tubes against corrosion in a wet, harsh geothermal environment. Furthermore, modifying the surfaces of the PPS top layer with PTFE, retarded the hydrothermal oxidation of the liner, thereby reducing significantly the rate of scale deposition and creating surfaces unsusceptible to reactions with scales. Thus, all the scales deposited on the liner's surfaces were readily scoured off by hydroblasting at a very low pressure. By contrast, although the stainless steel tubes had a great protection against corrosion, the formation of passive oxide layers at their outermost surface sites was detrimental in that they became more susceptible to scale deposition and developed strong adherence to the scales. As a result, the high-pressure hydroblasting was required to remove this scale adhering to the tubes' surfaces.

© 2002 Kluwer Academic Publishers

1. Introduction

As previously described [1–3], we designed and developed several poly(phenylenesulfide) (PPS)-based coating systems in geothermal material research program aimed at extending the useful lifetime of carbon steel heat exchanger tubes used in geothermal binary-cycle power plants operating at temperatures up to 160°C. The coating systems were required to have the following properties: (1) good thermal conductivity; (2) protection of steel tube against corrosion and oxidation; (3) anti-fouling characteristics; and, (4) resistance to abrasive wear. In the first criterion, the silicon carbide (SiC) grit was used as the thermally conductive filler and was packed into the PPS layer. SiC improves heat transfer by 16%, compared with that of unfilled PPS. For the second property, crystalline zinc phosphate (Zn.Ph) ceramic primer was directly deposited on the underlying steel surfaces. The Zn.Ph primer not only imparts cathodic protection to inhibit the corrosion

of steel, but also has a coupling function, strongly linking between the PPS coating and the steel substrate. In particular, the chemical reaction between Zn.Ph crystals and PPS led to the formation of zinc sulfide as the interfacial reaction product at critical interfacial boundary zone; this product confers outstanding adherence of the coating to the primer.

In readily transferring the heat energy generated by passing hot brine through the heat exchanger tubes, the coating's surfaces inevitably must possess anti-fouling characteristics. The scales that accumulate over the tubes' surfaces cause a loss in two important functions, the flow pressure of brine and the efficacy of heat transfer, in the heat exchangers. To restore these functions, the scale layers must to be scoured off from the tubes' surfaces. Among the technologies for removing scales, hydroblasting is most commonly used to clean the fouled tubes. However, the strong bond formed between the scales and the tubes' surfaces not only requires

highly pressurized hydroblasting, but also a substantial amount of time to dislodge them completely. Such scouring is time-consuming and very costly. Finally, the coating's surfaces also must be resistant to abrasive wear to abate damage from scratching brought about by the passage of fine hard mineral particles through the tubes, and by the impact of scale particles during hydroblasting. In trying to alleviate the wear damage, we incorporated hydraulic aluminum oxide-rich calcium aluminate (ACA) fillers into the PPS matrix. When the ACA fillers come in contact with hot brine at damaged sites in the coating, the Cl^- and SO_4^{2-} anions in brine react with the Ca^{2+} ions liberated from the ACA grains to form water-soluble CaCl_2 and CaSO_4 as the reaction products. After these reaction products are leached out from the damaged coating sites, the Ca-depleted ACA is transformed into crystalline boehmite ($\gamma\text{-AlOOH}$) phase, a well-known hard, tough, strong ceramic. Hence, the growth of boehmite crystals in a damaged polymer matrix significantly contributes to minimizing the rate of abrasive wear of the coatings' surfaces.

All the information described above was obtained from coupon test specimens exposed to a simulated geothermal environment in the laboratory. To ensure that the laboratory's results are duplicated in the field, we lined 6100-mm length carbon steel heat exchanger tubes with two different PPS-based coating systems. One system consisted of the zinc phosphate (Zn.Ph) primer, the SiC-filled PPS as the intermediate layer, and the PTFE-blended PPS as the top layer. The other was comprised of the Zn.Ph primer and the ACA-filled PPS only. The lined tubes were set into the test skids at the Mammoth geothermal power plant site, and were exposed for eleven months to flowing geothermal brine at temperature of 160°C.

Thus, the objective of the present study was to conduct post-test analyses of the exposed liners. The physicochemical factors to be analyzed included the chemistry of the scales deposited on the liner's surfaces, the interfacial bond between the liners and the scales, the chemical composition and state of liner's surfaces, the thermal properties, and the microprobe profile at liner/steel joints. Integrating these data would provide us with the information on the reliability of these liners in protecting the carbon steel heat exchanger tubes against corrosion, oxidation, and scaling in such a harsh, hostile geothermal environment. For comparison with these liners, we used the stainless steel tubes without any liners.

2. Experimental

2.1. Materials

The AISI 1008 carbon steel heat exchanger tubes, 6100-mm long, 25-mm outside diam. with 1.2-mm-thick walls, were lined with the coating materials. The reference stainless steel tube with as same dimension as that of the carbon steel tubes was AISI AL-6XN. The "as-received" PPS powder for the slurry coatings, supplied by Ticona (Summit, NJ, USA), had a particle size of $<20\ \mu\text{m}$ and a high melt flow at temper-

TABLE I Formulation of slurry systems

System	Composition (wt%)				
	PPS	SiC	ACA	PTFE	Isopropyl alcohol
SiC/PPS	36.0	19.0	–	–	45.0
ACA/PPS	45.0	–	4.5	–	50.5
PTFE/PPS	43.0	–	–	4.3	52.7

atures above its melting point of $\sim 250^\circ\text{C}$. The PTFE powder under the commercial trade name "SST-3H", supplied by Shammrock Technologies (Newark, NJ, USA), was used as a slip-enhancing and anti-oxidant additive to PPS, and had a particle size of $\sim 40\ \mu\text{m}$. PTFE-blended PPS powder, with a PPS/PTFE ratio of 90/10 by weight, was prepared in a rotary blender. Aluminum oxide-rich calcium aluminate (ACA), supplied by Lafarge Aluminates (Temecula, CA, USA), was used as the hydraulic filler. The ACA contained two major chemical constituents, 69.8–72.2% aluminium oxide and 26.8–29.2% calcium oxide. It had a surface area of 0.38–0.44 m^2/g , and a particle size of $<90\ \mu\text{m}$. An x-ray powder diffraction (XRD) survey of the ACA revealed that its main mineralogical composition consists of crystalline calcium dialuminate ($\text{CaO} \cdot 2\text{Al}_2\text{O}_3$) and calcium monaluminate ($\text{CaO} \cdot \text{Al}_2\text{O}_3$). The ACA filler, at 10% by weight of the total amount of PPS, was mixed with the PPS powder in a rotary blender. The silicon carbide (SiC) grits used to enhance the thermal conductivity of the PPS layer were a mixture of grits consisting of three different sizes, ~ 142 , ~ 32 , and $\sim 9\ \mu\text{m}$, obtained from Norton Corporation (Akron, OH, USA). The industrial grade isopropyl alcohol was used to make the slurries. Table I gives the formulations of the three different slurries, SiC-filled PPS, ACA-filled PPS, and PTFE-blended PPS, that were used to line the internal surfaces of the heat exchanger tubes. Before depositing these coatings on the interior surfaces of the tubes, the tubes' surface first were covered with a zinc phosphate (Zn.Ph) primer. The Zn.Ph primer was applied using a "fill and drain" technique. The tube was primed by attaching a valve to one end of it and then inserting it into a vertically oriented furnace. The priming solution consisting of 5.0 wt% zinc orthophosphate dihydrate, 10.0 wt% H_3PO_4 , 1.0 wt% $\text{Mn}(\text{NO}_3)_2 \cdot 6\text{H}_2\text{O}$, and 84.0 wt% water was poured into the tube from the top, and then drained from the bottom once the priming process was completed. The steps in this process are as follows: (1) insert the tube into the vertical furnace, (2) pre-heat the tube to 80°C, (3) pre-heat the Zn.Ph solution to 80°C, (4) fill the tube with the Zn.Ph solution and maintain it at $80^\circ\text{C} \pm 5^\circ$ for 30 min, (5) drain the solution from the tube and wash the interior with water, and, (6) heat the primed tube at 125°C for 1 hr to eliminate any moisture from the primer layer.

2.2. Lining technology

Table II shows two different coating systems used for lining the Zn.Ph-primed internal surfaces of the tubes. For both coating systems, the layers were deposited in accord with the following steps; we detail the steps for

TABLE II Coating systems for the Zn.Ph-primed internal surface of heat exchanger tubes

System	Coating layer		
	First	Second	Top
1	SiC/PPS	SiC/PPS	PTFE/PPS
2	ACA/PPS	ACA/PPS	ACA/PPS

No. 1 system. First, the primed tube was inserted into the vertical furnace. Second, the SiC-filled PPS slurry was poured into the tube until it was filled, and then it was slowly drained from the tube. Third, the slurry-lined tube was left for at least twelve hours to allow the alcohol to volatilize at room temperature. Finally, the tube was baked for 2 hours at 320°C to ensure the melt-flow of PPS, and then was cooled off to room temperature. This entire process, called “fill-drain-baking” then was repeated to superimpose the second coating layer of SiC-filled PPS slurry over the first one. After this, the top coating layer of PTFE-PPS was overlaid on this SiC-filled intermediate layer, using the same lining process.

The overall coating of system No. 2 consisted only of ACA-filled PPS slurry lying on the primer. The same fill-drain-baking technique was used and three layers of the slurry were applied. The thickness of these liners without the Zn.Ph primer (8 to 60 μm thick) ranged from 300 to 330 μm.

2.3. Measurements

Scanning electron microscopy (SEM) was used to explore the morphological features of the scales deposited on the surfaces of the exposed liners, and also to obtain insight into the microstructure of the cross-sectional

area at the liner/steel joints. The elemental composition accompanying the SEM image was detected by the energy-dispersive x-ray spectroscopy (EDX). To support the EDX data of the scales, disks for Fourier transform infrared (FT-IR) analysis were prepared by mixing 200 mg of KBr and 2 to 3 mg of scale samples collected from the surfaces of liners. Using strain-jet hydroblasting equipment with an injection nozzle of ~12.5 mm diam, the extent of the interfacial bonding force between the liners, or the stainless steel tubes and the scales was estimated from the hydropressure needed for scouring the scales off from the surfaces of each. X-ray photoelectron spectroscopy (XPS) was used to determine the changes in chemical composition and state at the surfaces of liners after exposure. Excitation radiation was provided by an AlKα(1486.6 eV) x-ray source, operated at a constant power of 200 W and in a vacuum in the analyzer chamber of $133.3 \times 10^{-9} \text{ Nm}^{-2}$. The changes in thermal properties including endothermic energy at the melting point, and exothermic energy at the crystallization temperature for the semi-crystalline PPS and PTFE thermoplastic matrices after the field test were surveyed by differential scanning calorimetry (DSC) in N₂. A cyclic DSC test over the temperature range of 25 to 350°C was run using the non-isothermal method at a heating-cooling rate of ±10°C/min.

3. Results and discussion

3.1. Scale deposition

Fig. 1 shows the SEM microphotograph of the scale deposited on the surfaces of the PTFE-blended PPS top layer. The image revealed the accumulation of flake-like scales covering the entire surface of the top layer.

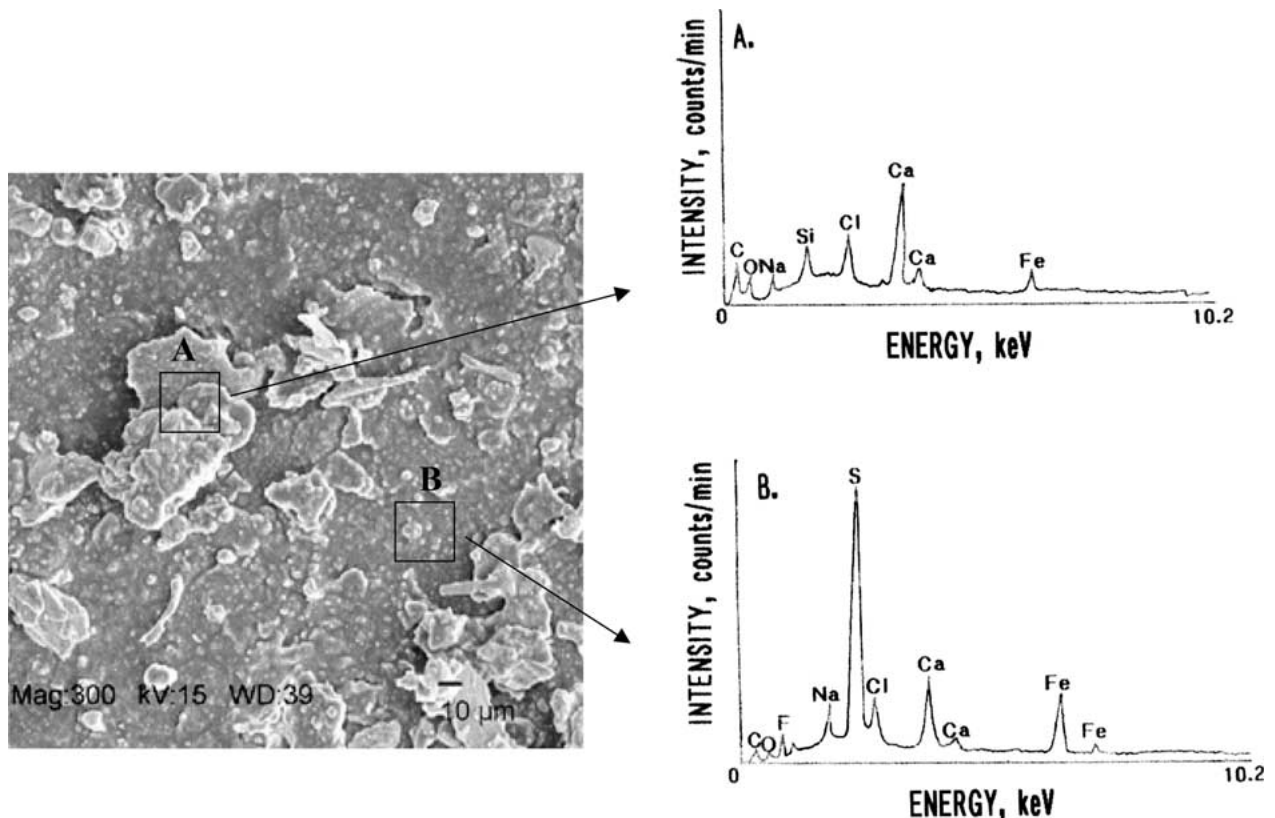


Figure 1 SEM microphotograph and EDX spectra of scale deposited on PTFE-blended PPS's surfaces after eleven-month-long field exposure.

The EDX spectrum of the scale fragments denoted as area "A" had seven elemental distributions, C, O, Na, Si, Cl, Ca, and Fe, as the representative elements of the scales. Among these elements, Na and Cl may be attributed to the NaCl salt, while possible assignments of three other elements, O, Ca, and Si, are the calcium silicate compounds and silica. The Fe-related components of scales may be associated with FeCl₂ and Fe oxides. The remaining component of the scales reflects organic contaminants because of the presence of a conspicuous C signal. The EDX spectrum from the other area marked as site "B" included a pronounced signal from the S element, moderately intense signals of Si, Cl, Ca, and Fe, and weaker signals from C, O, F, and Na. The major element S along with the F element appears to be originated from the PTFE-blended PPS coating. All the other elements seem to come from the scales. The EDX is extremely useful for the quantitative analysis of individual elements in a solid surface layer, up to ~1.5 μm thick because of the penetration of the electrons to that depth. Thus, it is possible to assume that the thickness of some scale layers is no more than 1.5 μm. To the contrary, the EDX spectrum (not shown) of the scales accumulated over the stainless steel tube do not show any typical elements like Cr, Mn, and Ni that are representative of the major chemical components of the stainless steel. This implies that the scale layer deposited on the stainless steel is more than 1.5 μm thick. This information strongly suggested that the susceptibility of the stainless steel's surfaces to the scale deposition is much greater than that of the surfaces of the PTFE-blended PPS liner.

To support the information on the chemical constituents of the scales, FT-IR analysis (Fig. 2) of powdered scales was carried out over the frequency range of 4500 to 450 cm⁻¹. The IR spectrum showed the following absorption bands at 3423 and 1627 cm⁻¹ attributed to O—H stretching and bending vibrations of H₂O, respectively, at 2923, 2853, and 1463 cm⁻¹, which can be

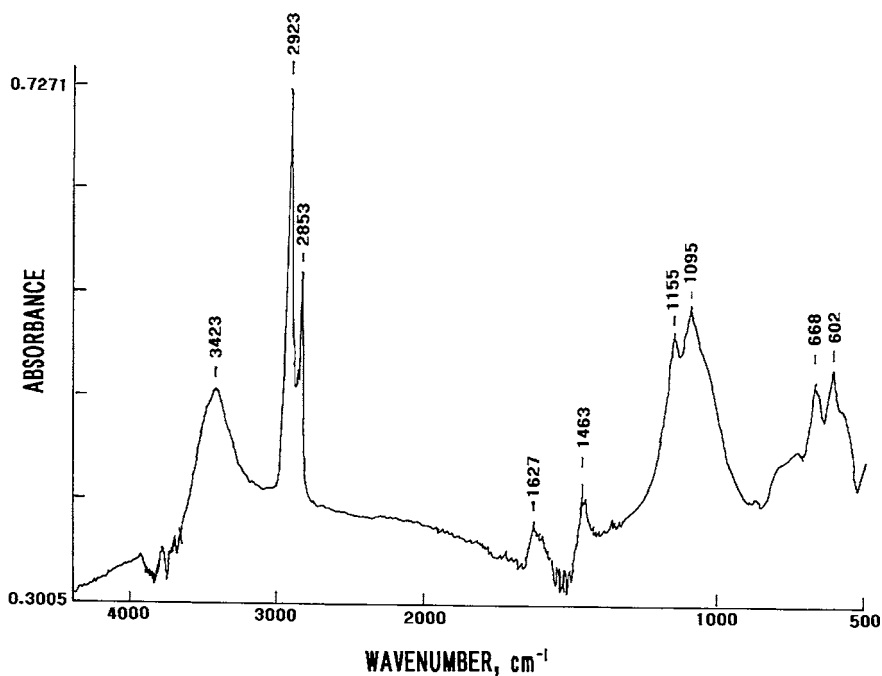


Figure 2 FT-IR spectrum of scale collected from the exposed liner's surfaces.

ascribed to the aliphatic C—H stretching and bending modes of CH₂ group, at 1155 and 1095 cm⁻¹, corresponding to the calcium silicate and silica [4, 5], and at 668 and 602 cm⁻¹, revealing the inorganic Cl-related salts [6]. From the presence of H₂O molecules, the calcium silicate might be defined as hydrated calcium silicate compounds. To ascertain further whether calcium silicate hydrate and silica were formed, we inspected the XPS Si_{2p} core-level photoemission spectrum excited from the scales' surfaces. In this spectrum, the scale of the binding energy (BE) was calibrated with the C_{1s} of the principal hydrocarbon-type carbon peak, fixed at 285.0 eV as an internal reference standard. A curve deconvolution technique, using a DuPont curve resolver, was employed to substantiate the information on the Si-related chemical states in the Si_{2p} region. The Si_{2p} core-level excitation curve (Fig. 3) had two resolvable Gaussian peaks at 102.6 and 103.4 eV. According to reference [7], the main peak at 102.6 eV as the principal Si-associated chemical state is due to the Si in the silicate compounds, and the shoulder peak at 103.4 eV originates from the Si in the silica (SiO₂). The results from FT-IR and XPS analyses clearly demonstrated that the scales mainly contained at least five

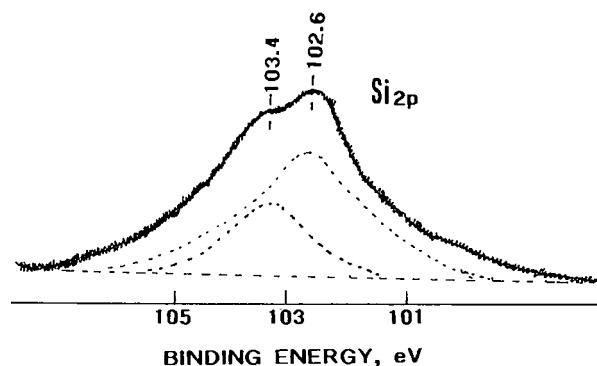


Figure 3 XPS Si_{2p} core-level photoemission spectrum of scale's surfaces.

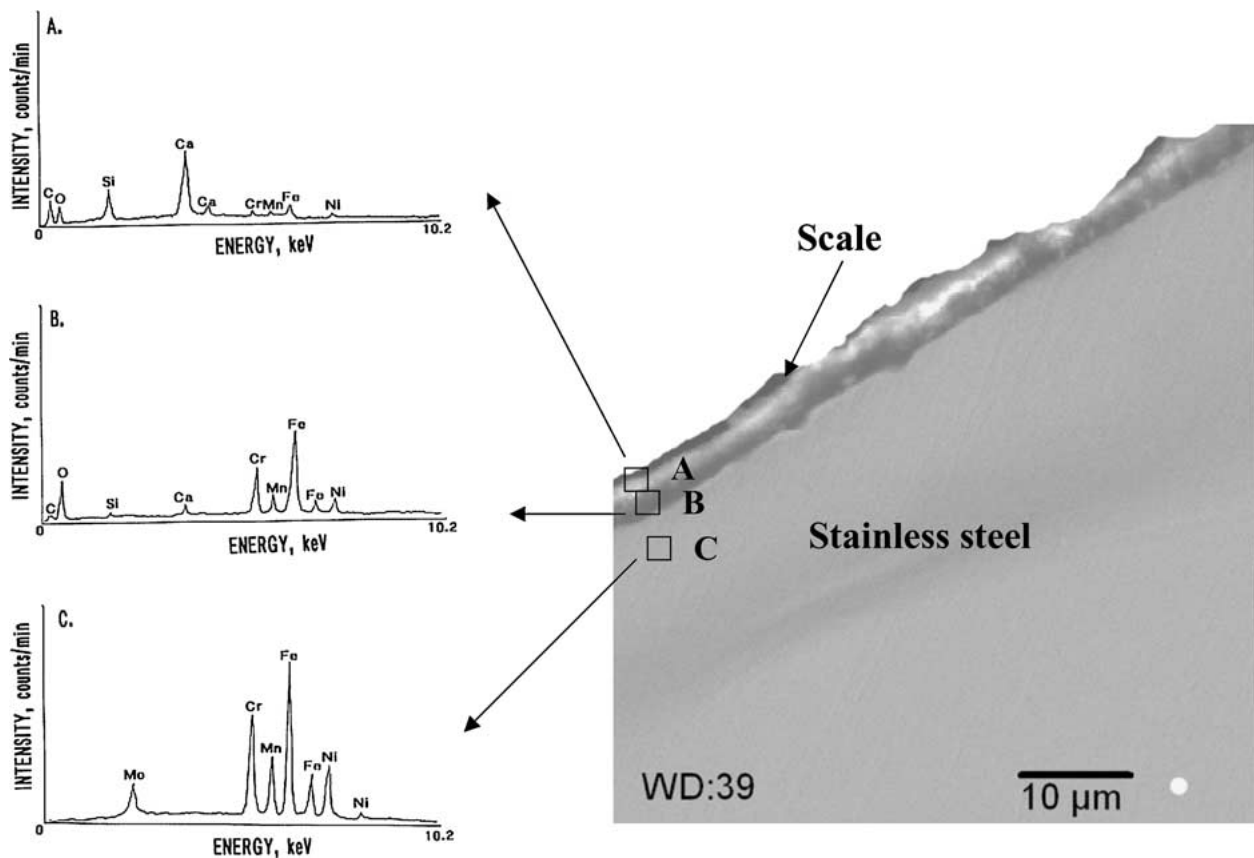


Figure 4 SEM image coupled with EDX analysis for cross-sectional area at critical interfacial region between stainless steel and scale after hydroblasting.

chemical components, organic contaminants, calcium silicate hydrate, silica, and Cl-associated salts.

Next, attention was focused on assessing how well the scale adheres to the tube's surfaces. We adapted the technique for hydroblasting to obtain this information. Thus, the extent of the adherence of the scales to the surfaces of liners and the stainless steel tube was estimated by determining the hydropressure needed for scouring all scales from the internal surfaces of the 6100 mm-long tubes. The results showed that the scales deposited on both the PTFE-blended PPS and ACA-filled PPS surfaces were easily removed by relatively low hydropressure, ranging from 10.3 to 13.8 MPa. By contrast, hydropressure as high as 55.1 MPa was required to dislodge the scales from stainless steel, clearly verifying that the scales adhere to the bare stainless steel much more firmly than they do to the liners. Furthermore, despite using such a high hydropressure, we recognized from a visual inspection that some scales still remained on the stainless steel surfaces. To obtain insight into the microstructure of the remaining scales, a cross-sectional area of the tube was explored by SEM (Fig. 4). As seen, the scale layer had a thickness of $\sim 5\mu\text{m}$ and was comprised of two different layers marked as "A" and "B". The SEM image revealed morphological features representing a strong bond between these two layers. The EDX spectrum of the top layer in the scale gave four strong signals from C, O, Si, and Ca, as the principal elements. The contributors to these elements are calcium silicate hydrate, silica, and organic contaminants. There were no Na and Cl

elements from salt, inferring that any salt compounds present in the original scales were washed away by hydroblasting. The EDX data of the bottom layer was characterized by three prominent peaks related to the O, Cr, and Fe elements, moderately intense Ca, Mn, and Ni peaks, and weak C and Si signals. As shown by EDX, stainless steel has five major elements, Mo, Cr, Mn, Fe, and Ni. Hence, the source of these four elements that were detected in the bottom layer appears to be the stainless steel. Relating these metal elements to the marked signal of O element, we assumed that these metals occupying the outermost surface sites of the steel were oxidized during its exposure. If this interpretation is valid, these metal oxide layers that formed over the steel surfaces have some affinity for calcium silicate and silica scales, thereby forming a strong interfacial bond between the metal oxide and the scales. This is a main reason why scales deposited on the stainless steel were very difficult to scour away.

In contrast, the scales over the PTFE-blended PPS surfaces were flaked off readily by low-pressure hydroblasting. Compared with the SEM image (Fig. 1) from a surface fouled by scale deposits, a dramatic change can be seen after hydroblasting (Fig. 5); namely, there are no remnants of any scales. In fact, the EDX analysis did not detect any scale-related elements, such as Ca, Si, Na, Cl, and Fe, demonstrating that the surfaces of PTFE-blended PPS liner are insensitive to reactions with the scales. This means that the extent of the interfacial bonding force between the liner and the scale is minimal, if any. The SEM image

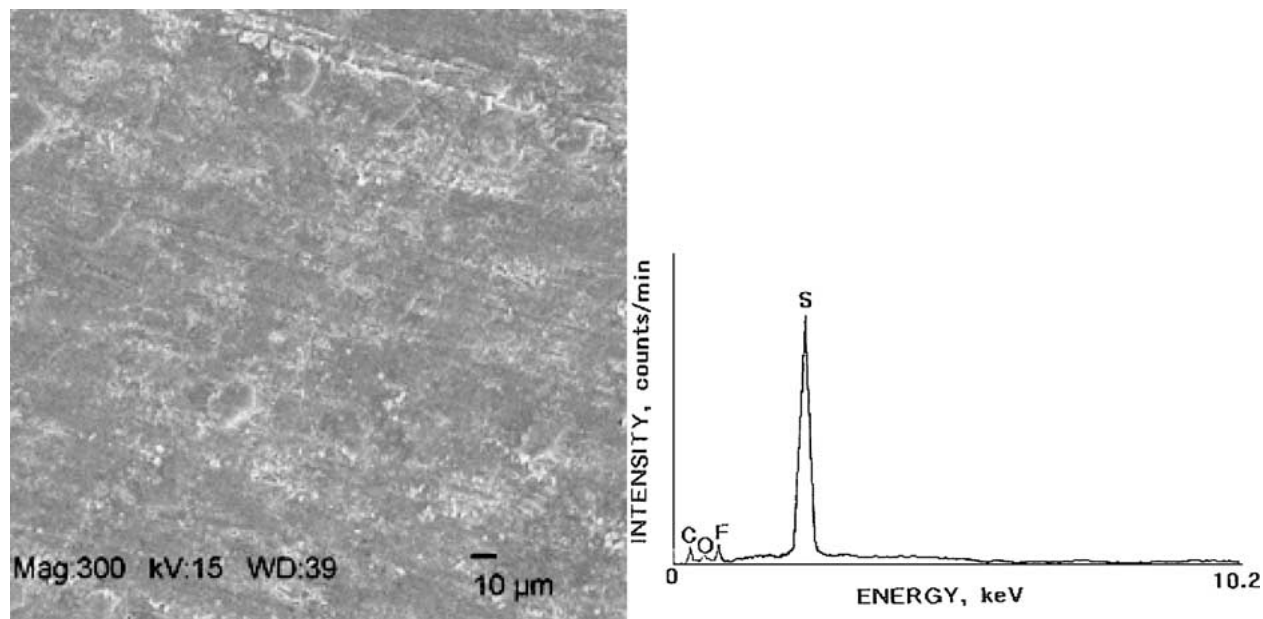


Figure 5 SEM-EDX analysis of PTFE-blended PPS's surface after hydroblasting.

(not shown) of the surfaces of the ACA-filled PPS liner after hydroblasting showed no significant differences to that of unexposed surfaces. Also, SEM exploration revealed no signs of any surface damages brought about by hydroblasting. However, although the signal intensity was very weak, the EDX (not shown) indicated the presence of Si which is one of the scale-related elements. Relating this Si signal to the O signal that also was detected, a possible interpretation is that some silica seems to remain on the hydroblasted liner's surfaces.

3.2. Liner's surfaces

To understand why the PPS liner's surfaces without the PTFE become susceptible to the deposition of silica scales during exposure, we investigated the changes in chemical composition of the hydroblasted liner's surfaces after exposure, compared with that of the unexposed ones. The surfaces for the PTFE-blended PPS and ACA-filled PPS liners before and after exposure were analyzed using XPS. All XPS measurements were made at an electron take-off angle of 40°, which corresponds to an electron-penetration depth of ~5 nm, reflecting the detection of atomic fraction and chemical states present in a superficial layer with a thickness of ~5 nm. Table III gives the XPS atomic fractions of all chemical elements detected on the surfaces of liners.

TABLE III Atomic composition of the surfaces of liners before and after 11-mo.-long field exposure test

Liner	Field test	Atomic fractions (%)					Atomic ratio (O/C)
		Si	S	C	O	F	
PTFE-blended PPS	Before	0.0	2.1	48.0	2.6	47.3	0.054
PTFE-blended PPS	After	0.0	1.3	48.8	3.1	46.8	0.064
ACA-filled PPS	Before	0.0	13.1	81.6	5.3	0.0	0.065
ACA-filled PPS	After	0.4	9.9	76.9	12.8	0.0	0.167

The quantitative data for the respective chemical elements were estimated by comparing the XPS Si_{2p}, S_{2p}, C_{1s}, O_{1s}, and F_{1s} core-level areas, which were then converted into atomic concentrations. Before exposure, the atomic fraction of PTFE-blended PPS's surfaces consisted of two dominant atoms, 48.0% C and 47.3% F, and two minor ones, 2.6% O and 2.1% S. The source of F and C atoms is the PTFE. Thus, we believe that the superficial layer (no more than 5 nm thick) was made up almost exclusively of PTFE. This phenomenon was due to the typical separation of PTFE from PPS and its migration upwards to the top surface of the liner. Consequently, PTFE occupied the liner's outermost surface site. By comparison, no conspicuous difference in the atomic fraction was obtained from the exposed liner's surfaces. Although some oxygen was incorporated in the superficial layer, its amount was negligible.

The ACA-filled PPS liner's surfaces were comprised of 13.1% S, 81.6% C, and 5.3% O. No ACA-related atoms, such as Al and Ca, were detected, reflecting the coverage of the entire surfaces of all ACA grains by a PPS layer, at least 5.0 nm thick. For the surfaces of the exposed liner, our attention was centered on incorporating a substantial amount of oxygen into the top surface layer. The atomic ratio of O/C of the exposed liner rose 2.6 fold to 0.167 compared to the unexposed one. This can be taken as evidence that the PPS's surfaces underwent some degree of hot brine-catalyzed oxidation. The data also indicated that 0.4% Si atom was incorporated into the superficial layer. Thus, the oxidation products formed at outermost surface sites seem to have an undesirable function similar to that of the oxide compounds accruing on stainless steel's surfaces; namely, they are sensitive to silica deposition. From the above information, PTFE as the anti-oxidant additive of PPS appears to play an essential role in reducing the rate of the scale deposition and in creating an inert surface to reactions with the scale.

To identify the oxidation products of PPS surfaces, XPS S_{2p} region for the ACA-filled PPS liner's surfaces

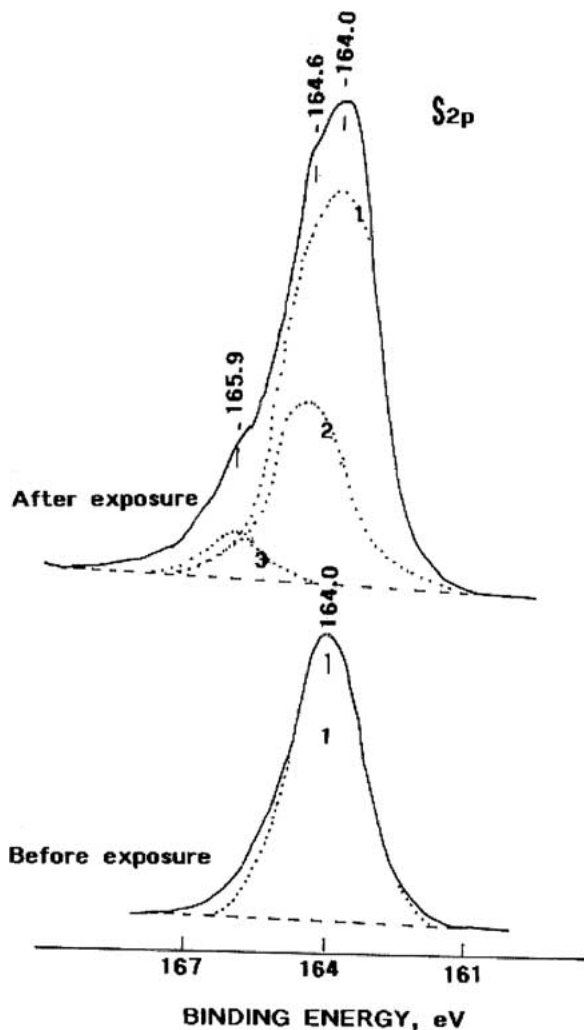
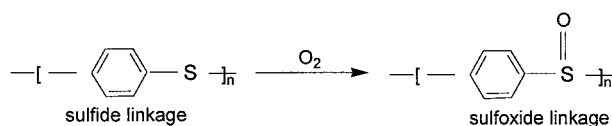


Figure 6 XPS S_{2p} region for the ACA-filled PPS liner's surfaces before and after exposure.

before and after exposure was inspected (Fig. 6). The spectral feature of the unexposed surfaces indicated the symmetrical peak that represents the presence of single sulfur compound. The single excitation at 164 eV deconvoluted as the area No.1 revealed the sulfide S in PPS [9]. The spectrum of the exposed liner included two additional peaks at 164.6 and 165.9 eV accompanying the areas No. 2 and 3, while the sulfide S peak at 164 eV still remained as the principal component. The possible contributions to the excitation at 164.6 and 165.9 eV are the S in the disulfide ($-S-S-$) and the sulfoxide ($>S=O$) groups, respectively [9, 10]. To account for the generation of a sulfoxide group, we believe that the hydrothermal oxidation of PPS led to the incorporation of oxygen into its molecular structure, so substituting bridging sulfide linkages for the sulfoxide-type linkages:



Conceivably, the sulfide \rightarrow sulfoxide substitution might transfer the non-functional surface of the liner into a functional one, which acts to initiate the deposition of scales.

3.3. Microprobe profiling

Next, our focus was directed toward exploring the cross-sectional areas of the liner layer and the critical interfacial boundary regions to ensure that the coating systems adequately protect the underlying steel tube against corrosion. Fig. 7 gives the SEM microprobe profiling coupled with the EDX analysis for the coating system consisting of the Zn.Ph primer, SiC grit-filled PPS intermediate layer, and PTFE-blended PPS top layer. The EDX spectrum in area "A" contains prominent signals of Zn and P elements, representing a rough crystalline layer of the Zn.Ph primer superimposed on the steel surfaces. The image also revealed that melted PPS penetrates into the open surface microstructure and microfissures of Zn.Ph layer. Although there is no experimental evidence, such an anchoring effect of PPS in filling the spaces in the primer layer would increase the strength of the mechanical bond between the PPS and the Zn.Ph layers, thereby improving interfacial bond durability. The EDX spectrum from the site "B" location, $\sim 100 \mu\text{m}$ away from the top surface, included the four elements, S, Si, O, and C. The Si along with some C belongs to the thermally conductive SiC grits distributed randomly in the PPS matrix accompanying the dominant signal of the S element. In the top layer of $\sim 40 \mu\text{m}$ thick without SiC grits, the area "C" at a distance of $\sim 20 \mu\text{m}$ beneath the surface exhibited the typical EDX spectral features of PTFE-blended PPS. This spectrum showed no traces of Na and Cl, demonstrating that no brine had penetrated through the lining layer. As a result, this 11-mo.-old coating system satisfactorily withstood the 160°C brine and adequately protected the underlying steel tube against corrosion in a wet, harsh geothermal environment.

Fig. 8 shows the SEM microphotograph and EDX spectra for the profile of the ACA-filled PPS liner/Zn.Ph/steel joints. The SEM image disclosed the outstanding performance of the liner in protecting the tube against corrosion. There is no sign of any internal delamination of the liner from the steel, nor were any blisters generated at the critical interfacial region between the ACA-filled PPS and the Zn.Ph. This can be taken as evidence that the interfacial bonding structure at the PPS coating/Zn.Ph primer/steel joint is satisfactorily stable and durable (see the SEM enlargement of square area). The image also revealed that the ACA grains were uniformly distributed in the PPS matrix, reflecting a good wetting behavior of ACA surfaces by molten PPS. In the area "A", the EDX contained a very intense signal of Al, a moderate Ca signal, and minor S and O signals, representing the coverage of the ACA grains by PPS. Like the PTFE-blended PPS top layer, no brine-related elements, such as Na and Cl, were detected in the area "B", $\sim 5 \mu\text{m}$ away from the liner's surfaces. It is clear that the ACA-filled PPS coating did not allow any hot brine to permeate through the lining layer during the 11-mo. exposure.

3.4. Thermal stability

Although these liners imparted an outstanding protection of the carbon steel tubes against corrosion, one

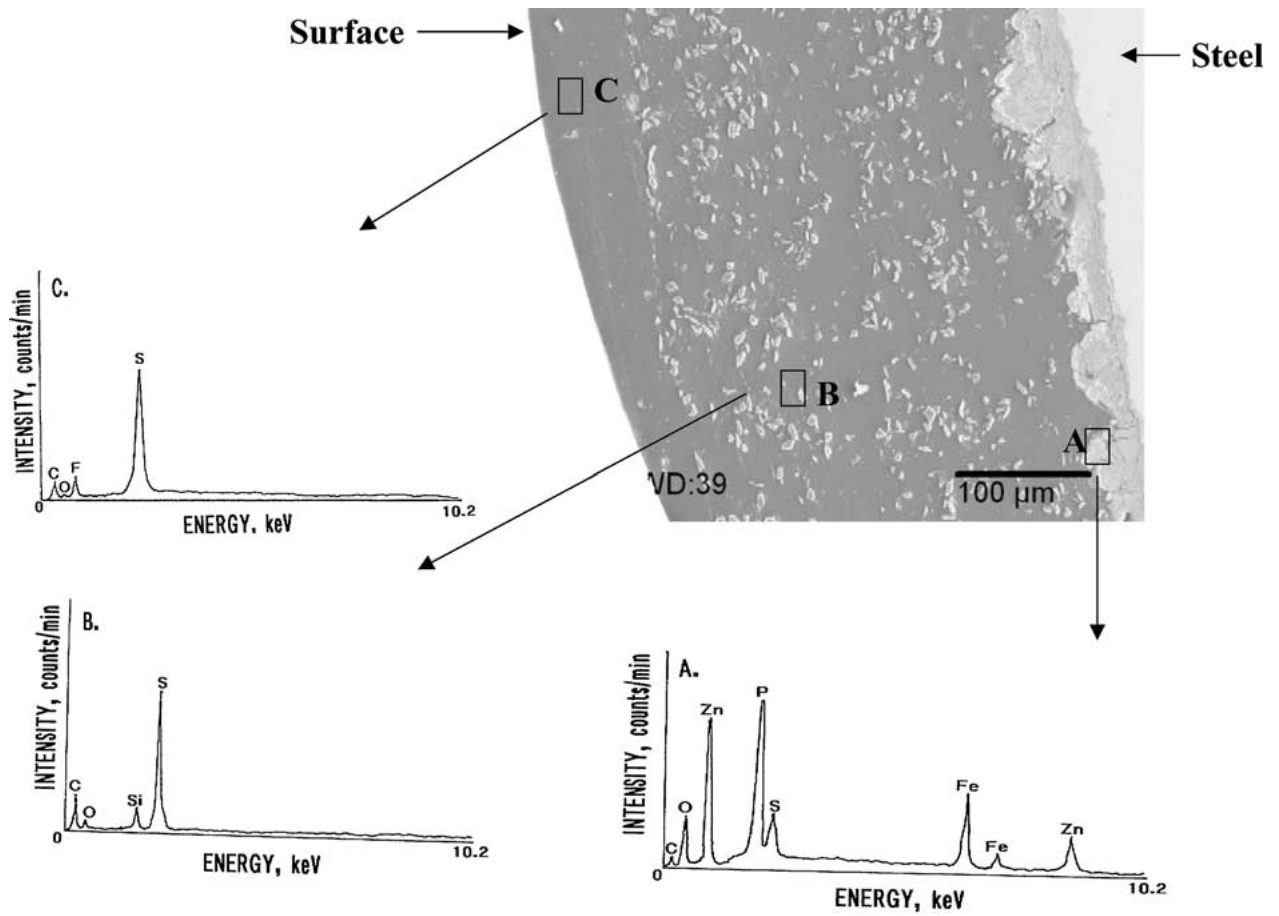


Figure 7 Microprobe profiling of hydroblasted PTFE-blended PPS/SiC-filled PPS/Zn.Ph primer lining system after 11-mo-long field exposure.

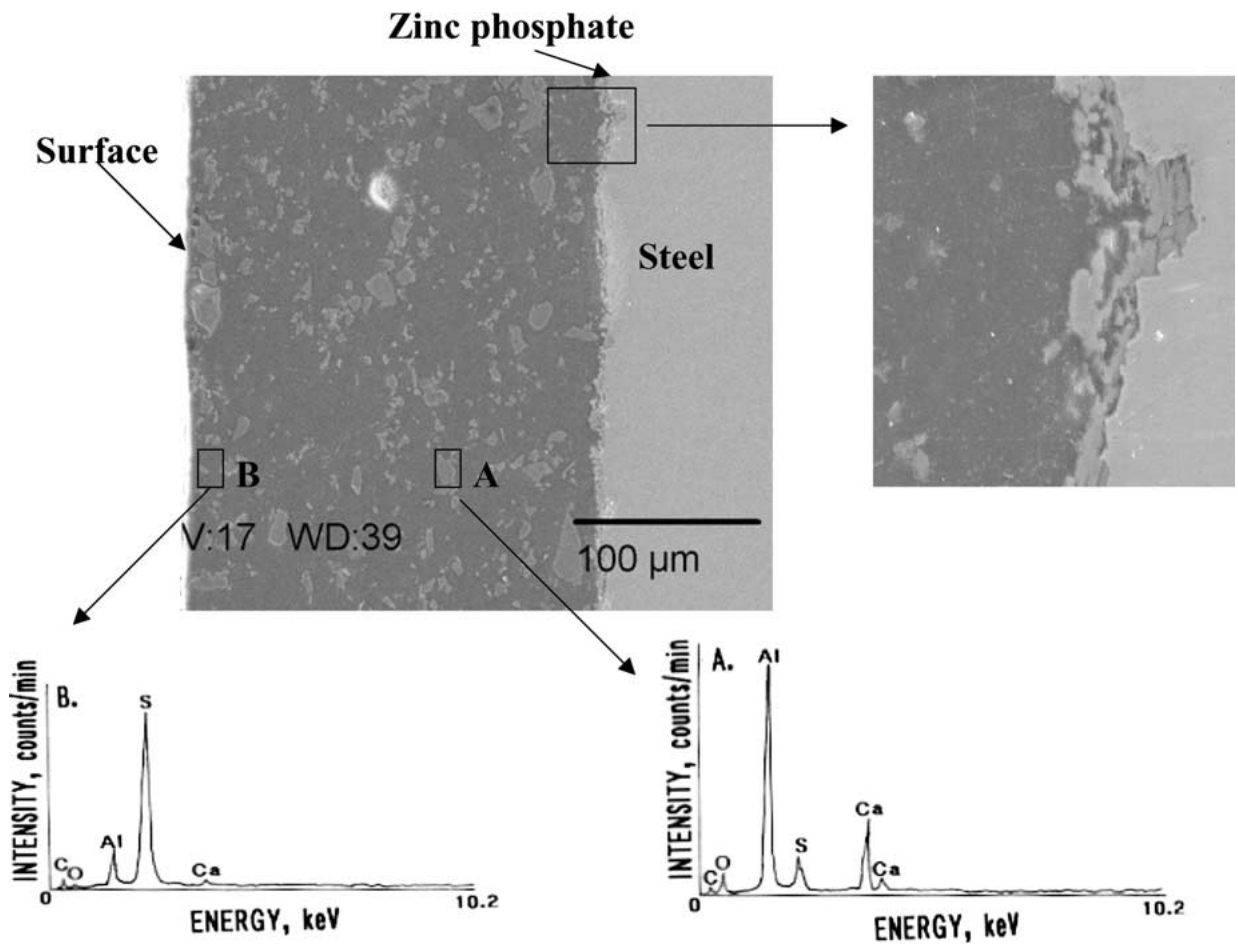


Figure 8 SEM-EDX exploration of the profile of hydroblasted ACA-filled PPS/Zn.Ph lining system after exposure.

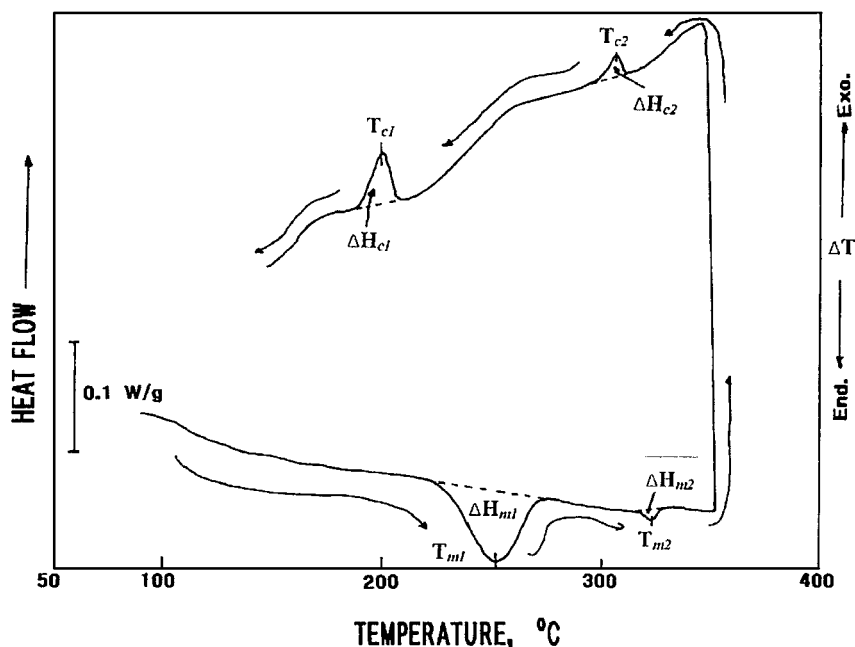


Figure 9 Cyclic DSC curve for the PTFE-blended PPS/SiC-filled PPS coating system.

important question remained unanswered: Do the thermal properties of these liners, such as the melting and crystallization temperatures, change after exposure? If a striking change occurred, attention then would have to be paid to a possible hydrothermal degradation of the coatings. To obtain this information, we determined the DSC endothermic melting and exothermal crystallization energies of the fragments of coatings removed from the unexposed and exposed tube's surfaces. The samples were prepared as follows: Open aluminum DSC pans were filled with ~3 mg fragments of the coatings. The pans were then sealed with aluminum covers for DSC analysis. The single PPS and PTFE-blended PPS thermoplastic polymers have the repeated melting-crystallization behaviors. Hence, we recorded the cyclic DSC curve of these polymers at the temperature range of 25 to 350°C. The typical cyclic DSC curve for the coating system consisting of PTFE-blended PPS and SiC-filled PPS is illustrated in Fig. 9. This thermodynamic DSC scan had two endothermic phase transition peaks, T_{m1} and T_{m2} , at ~250°C and ~320°C, attributed to the melting points of PPS and PTFE, respectively [2]. On cooling the two melted different polymers, two exothermic transition peaks, T_{c1} and T_{c2} , appeared around 200° and 310°C, which are due to the crystallizing temperatures of PPS and PTFE, respectively [2]. Correspondingly, the closed area of either the endothermic or exothermal curves with the baseline represents the total heat energy, ΔH , evolved during its melting or crystallizing. Thus, comparing the ΔH values of the unexposed coatings with that of exposed ones provides data on the extents of melting and crystallinity. The ΔH was computed using the following formula [11, 12]: $\Delta H = TRA/hm$, where T , R , A , h , and m refer to the temperature scale (°C mm⁻¹), the range sensitivity (4.18 mJ s⁻¹ mm⁻¹), the peak area (mm²), the heating rate (°C s⁻¹), and the sample's weight (mg), respectively.

TABLE IV Thermal properties of liners before and after field exposure

Coating system	Field test	Endothermic melting energy (J/g)		Exothermic crystallization energy (J/g)	
		ΔH_{m1}	ΔH_{m2}	ΔH_{c1}	ΔH_{c2}
PTFE-blended PPS/SiC-filled PPS	Before	10.40	0.32	3.38	0.55
PTFE-blended PPS/SiC-filled PPS	After	10.55	0.28	3.43	0.56
ACA-filled PPS	Before	14.40	—	5.10	—
ACA-filled PPS	After	14.43	—	4.99	—

Table IV lists the endothermic energies, ΔH_{m1} and ΔH_{m2} , generated at the melting points of PPS and PTFE, and the exothermic crystallization energies, ΔH_{c1} and ΔH_{c2} , of PPS and PTFE for the coating systems before and after exposure. For the coating system including PTFE-blended PPS and SiC-filled PPS, the PPS phase in the unexposed coating evolved the melting energy, ΔH_{m1} , of 10.40 J/g and the crystallizing energy, ΔH_{c1} , of 3.38 J/g. The weight proportion of PTFE to PPS was 1 to 26.7. This is the reason why the ΔH_{m2} and ΔH_{c2} values of PTFE in the same unexposed coating were considerably lower than those of the PPS. By comparison, no significant difference in these energies was determined from the exposed coating, strongly demonstrating that the coating system has an excellent hydrothermal stability. Likewise, the hydrothermal stability of the ACA-filled PPS coating was very good. In fact, when the ΔH_{m1} and ΔH_{c1} of the exposed PPS were compared with those of the unexposed one, there was no striking difference between them.

4. Conclusion

In trying to protect carbon steel heat exchanger tubes against corrosion and fouling by calcium silicate hydrate and silica scaling in geothermal binary-cycle power plants operating at a brine temperature of 160°C, their internal surfaces were lined with two high-temperature performance coating systems. The lined tubes then were exposed for eleven months at the Mammoth power plant site to ensure that these coating systems satisfactorily solved these problems facing the geothermal energy industry. One of these coating systems was comprised of three different coating layers, crystalline zinc phosphate (Zn.Ph), silicon carbide (SiC)-filled poly(phenylenesulfide) (PPS) as the intermediate layer, and polytetrafluoroethylene (PTFE)-blended PPS as the top surface layer. The other consisted of the Zn.Ph primer and aluminum oxide-rich calcium aluminate (ACA)-filled PPS layer. AISA AL-6XN stainless steel tubes also were used as the reference bare steel. Based upon the results from the post-test analyses of these liners after the eleven-month field exposure, the following general conclusions can be drawn:

1. Stainless steel tube is well protected against corrosion due to the formation of passive Cr, Fe, and Mn oxide layers at its outermost surface sites. However, these oxide layers are susceptible to reactions with calcium silicate hydrate and silica scales, thereby developing a strong adherence to the scale. This strong bond is reflected in the requirement for high-pressure hydroblasting of 55.1 MPa to scour them off from the tube's surfaces. But, even then, many scales forming a $\sim 2.0 \mu\text{m}$ thick layer still remained on the oxide layer after hydroblasting.

2. By contrast, the surfaces of a PPS top layer modified with PTFE as an anti-oxidant additive significantly retarded the hydrothermal oxidation of the liner. Such an anti-oxidant surface not only minimized the rate of the scale deposition, but also made it inert to reactions with the scales. Thus, all the scales deposited on the liner's surfaces were easily removed by hydroblasting with only ~ 18.0 MPa pressure. In addition, the PPS satisfactorily withstood a 160°C brine temperature and displayed a great resistance to the permeation

of brine through the liner, expressing an outstanding performance in protecting the tubes against corrosion.

3. The ACA-filled PPS liner's surfaces without the PTFE suffered some degree of the oxidation, causing the formation of a few silica scales on the hydroblasted liner's surfaces. However, there was no internal delamination of the PPS liner from the Zn.Ph primer, nor were any blisters generated in the critical interfacial boundary region between the PPS and the Zn.Ph primer. Furthermore, brine-related elements were not detected in a superficial layer of $\sim 5 \mu\text{m}$ thick, strongly demonstrating that although the ACA filler was incorporated, this liner adequately prevented corrosion of the tubes.

Acknowledgment

This program report, issued by Raymond LaSala (Program Manager, DOE Office of Wind and Geothermal Technologies), was performed under the auspices of the U.S. Department of Energy Washington, D.C. under Contract No. DE-AC02-98CH10866.

References

1. T. SUGAMA and N. CARCIELLO, *J. Coat. Tech.* **66** (1994) 43.
2. T. SUGAMA, *Polym. & Polym. Comp.* **6** (1998) 373.
3. T. SUGAMA and P. HAYENGA, *ibid.* **8** (2000) 307.
4. V. C. FARMER and J. D. RUSSELL, *Spectrochim. Acta* **20** (1964) 1149.
5. A. A. KLINE, M. E. MULLINS and B. C. CORNILSEN, *J. Am. Ceram. Sci.* **74** (1991) 2559.
6. K. NAKANISHI and P. H. SOLOMON, in "Infrared Absorption Spectroscopy" (Holden-Day, San Francisco, 1977) p. 56.
7. C. D. WAGNER, D. E. PASSOJA, H. F. HILLERY, T. G. KINISJY, H. A. SIX, W. J. JANSEN and J. A. TAYLOR, *J. Vac. Sci. Technol.* **21** (1982) 933.
8. J. RIGA, J. P. BONTIQUE, J. J. PIREAUX and J. J. VERBIST, in "Physicochemical Aspects of Polymer Surfaces," edited by K. L. Mittel (Plenum Press, New York, 1983) p. 45.
9. B. J. LINDBERG, K. HAMRIN, G. JOHANSSON, U. GELIUS, A. FAHLMAN, C. NORDLING and K. SIEGBAHN, *Physical Scrip.* **1** (1970) 286.
10. J. RIGA and J. J. VERBIST, *J. Chem. Soc. Perkin Trans.* **II** (1983) 1545.
11. C. S. RAY, W. HUANG and D. E. DAY, *J. Amer. Ceram. Soc.* **74** (1991) 60.
12. K. F. KELTON, *ibid.* **75** (1992) 2449.

Received XXXX

and accepted 21 March 2002